International Journal of Impact Engineering 109 (2017) 253–263

Contents lists available at ScienceDirect

International Journal of Impact Engineering

journal homepage: www.elsevier.com/locate/ijimpeng

# Numerical investigation into the stress wave transmitting characteristics of threads in the split Hopkinson tensile bar test

Khac-Ha Nguyen[a], Hee Cheol Kim[a], Hyunho Shin[b], Yo-Han Yoo[c], Jong-Bong Kim[a,*]

[a] Department of Automotive Engineering, Seoul National University of Technology, Gongneung-ro 232, Nowon-Gu, Seoul, 01811, South Korea
[b] Department of Materials Engineering, Gangneung-Wonju National University, 7 Jukheon-ghil, Gangneung, Gangwon-do, 25457, South Korea
[c] Agency for Defense Development, Yuseong, Daejeon, 34186, South Korea

ARTICLE INFO

*Article History:*
Received 19 December 2016
Revised 2 July 2017
Accepted 4 July 2017
Available online 5 July 2017

*Keywords:*
Split Hopkinson tensile bar
High strain rate
Finite element method
Thread design
Calibration specimen

ABSTRACT

The Split Hopkinson tensile Bar (SHTB) is one of the most widely used methods to study various material behaviors under tensile loading and high nominal strain rate. Since the specimens and grips with thread may disturb the wave propagation between bars and specimen, the stress-strain relation of the specimen, which is calculated from the strains of the incident and transmitter bars, may not match with the stress-strain relation measured directly from the specimen. In order to ensure a high accuracy of SHTB system, specimen calibration is usually carried out. To ensure the no wave distortion in the thread region, the stress wave should be entirely transmitted from the incident bar to the transmitter bar in tests using the calibration specimen (not the real specimen) of the same material and the same diameter with the transmitter and incident bars. Therefore, the strain signals at the incident and transmitter bars need to be the same. This study investigated the wave transmit characteristics through threads in SHTB test. To investigate the effect of the thread on the wave transmission, a specimen with the same diameter of the incident and the transmitter bars is used in the SHTB test. The effects of the thread inner diameter, yield stress, thread type, and strike velocity on the wave propagation characteristics are investigated. Based on the analysis results for various conditions, a proper design guide for a thread shape to secure the measurement accuracy in the SHTB test is proposed.



## 1. Introduction

The split Hopkinson bar (SHB) technique, first introduced by Kolsky [1], is one of the most widely used methods to study material behaviors under high nominal strain rate in a range of $10^2$–$10^4$ $s^{-1}$. In general, SHB methods are classified into torsion (SHToB) [2], compression (SHPB) and tension (SHTB) [3–9] split Hopkinson bars. Recently, tensile SHTB test are widely used to measure the tensile stress-strain relation [3–9]. The SHB tests can be approximately categorized into direct [2] and indirect [3–9] methods. Fig. 1 shows schematic illustration of the indirect tensile SHB test. In the same way to the SHPB test, the SHTB test apparatus, shown in Fig. 1, is consists of a striker bar, incident and transmitter bars, and a specimen. In this technique, a short material specimen is sandwiched between the incident and transmitter bars. Since a striker is fired at an incident bar, upon impact a stress wave propagates along the incident bar. At the end of the incident bar, a part of the stress flow is reflected back because of the impedance mismatch between the bars and specimen. A part of the stress flow keeps travelling along the specimen and the transmitter bar until it reaches the end of the bar. The deformation and load in the specimen are determined by measuring the stress wave flows in the bars, which remain elastic during the experiment.

Specimen and grip shapes were investigated to obtain high measurement accuracy for the SHTB system. Lindholm and Yeakley [6] performed tensile tests with hat type specimens. Although the test was easy to perform, the design of the hat type specimens was complicated and expensive. Huh et al. [7] and Pham et al. [8] used bolts to fix sheet type specimen into the bars. Pham et al. [8] investigated the errors caused by bolt type fixing. Nicholas [9] used threaded specimens to obtain high nominal strain rate stress-strain curves for over 20 different materials. In these experiments, however, the reliability of the wave transmission through the specimen threaded region was not verified.

Fig. 2 shows examples of measurement accuracy in SHTB. Fig. 2 (a) shows detailed view of assembled specimen and bars, utilizing a screw fixing. Specimen dimensions are shown in Fig. 2(b). Fig. 2(c) and (d) show examples of the measurement error caused by improper specimen design. Fig. 2(c) and (d) also show the comparison of the calculated (using the incident and transmitter bar strain)

* Corresponding author.
*E-mail addresses:* hshin@gwnu.ac.kr (H. Shin), jbkim@seoultech.ac.kr, jbkim@snut.ac.kr (J.-B. Kim).

http://dx.doi.org/10.1016/j.ijimpeng.2017.07.004
0734-743X/

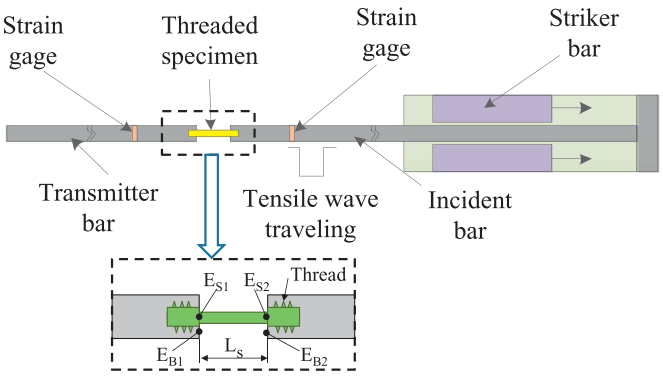


**Fig. 1.** Schematic illustration of the SHTB system.

stress-strain relation with that obtained directly from the specimen. It is difficult to measure the stress directly from the specimen; therefore, the validation of the measured stress is also difficult. In this study, a full 3-dimensional numerical experiment using the well-known commercial software, ABAQUS/Explicit, is carried out to validate the accuracy of the SHTB test results. The analysis model for SHTB test consists of a striker bar, incident and transmitter bars, and a specimen. The interaction between each part is treated by surface to surface contact. Initial velocity condition is imposed to the striker bar, and the strains at the incident and transmitter bars are monitored. In the finite element analysis, the stress and strain of the specimen can be monitored and the numerically measured stress and strain can be validated using the monitored value. Fig. 2(c) and (d) show the results for specimen diameters of 2.0 and 8.0 mm, respectively. In this analysis, the length and diameter of the incident and transmitter bars are 2000 mm and 16 mm, respectively. As can be seen in Fig. 2(c) and (d), the stress-strain relation is measured accurately when the specimen diameter is 8.0 mm, while a large discrepancy between the measured and monitored curves is shown when the specimen diameter is 2.0 mm. The proper design of the specimen shape, therefore, is very important. The only difference between the SHPB and SHTB is the fixing structure including thread. Therefore, it is considered that the wave is corrupted while passing the fixing structure including threads in incident bar, transmitter bars, and specimen. To confirm the stress equilibrium on the specimen, axial stress is monitored at the elements $E_{S1}$ and $E_{S2}$ (see Fig. 2(b), left and right ends of the specimen) and shown in Fig. 2(e) and (f). Before the first drop of the axial stress near 0.5 ms, the stress equilibrium is almost satisfied. After the drop of the axial stress, stress equilibrium is not satisfied and this is considered due to the different cross-section area by necking. Therefore, it is considered that the stress equilibrium is satisfied before necking.

The abrupt change of the cross-section may cause necking in early stage of tensile test. However, in the specimen that has smooth changing cross-section, it is difficult to define the deforming length '$L_s$'. This issue will be investigated in the later works of specimen design. In this work, only the wave propagation characteristics in the thread region will be investigated.

To confirm the stress transmitting characteristics through the threads, Naik and Perla [10] and Pothnis et al. [11] carried out a calibration test using a specimen with a diameter identical to those of the incident and the transmitter bars. In their test, the striker velocity was very low at about 6 m/s. As will be discussed in the main text, the stress wave can be transmitted without distortion through the thread when the strike velocity is low. However, severe wave distortion takes place when the striker velocity is high. Therefore, the proper striker velocity and specimen shapes, including the shape of the thread, should be designed to prevent wave distortion in the thread region.

In order to avoid error caused by the fixing structure of the specimen, Vilamosa et al. [12] used a high-speed camera to measure the local strain directly from the specimen and monitor the fracture processes in high strain rate tests. The advantage of this method is the measurement of the material beyond necking or fracture for some materials, such as glass, stone, etc. However, this technique is very complicated and expensive. Haugou et al. [13] proposed a new grip structure for the SHTB to measure the stress-strain relation of a sheet metal specimen and to investigate the influence of the grips on the elastic wave propagation. Fransplass et al. [14,15] studied the tensile behavior of threaded steel fasteners at high strain rate deformation. They showed that the force equilibrium is satisfied when the stress wave passes through the thread region. While the force equilibrium is satisfied, the stress and strain, which are calculated using one-dimensional stress wave theory, may contain error due to plastic deformation of the thread region. As will be discussed in Section 3.3, all of the specimen regions except the specimen center (marked by 'Ls' in Fig. 2(b)) should remain in an elastic state for accurate measurement. Chen et al. [16,17] also measured the tensile stress-strain relation at high nominal strain rate using the SHTB. They used non-uniform specimens and corrected the strain error caused by non-uniform diameter of the specimen.

For the compressive SHB test, Chen et al. [18] investigated the effect of specimen length to diameter ($L_s$/D) on the measurement accuracy. In SHPB test, the ratio of length to diameter is a well-known parameter to obtain good signal. In SHTB test, also, the ratio of length to diameter of the specimen is a main design parameter. Moreover, the thread design is also very important to get an accurate result in SHTB test. So, only the wave propagation characteristic is investigated in this work. The specimen design (including dumb-bell and uniform cross-section specimen) will be carried out later.

In this study, as a preliminary work for the specimen shape design, the wave transmitting characteristics of thread are investigated. As was done in the studies of Naik and Perla [10] and Pothnis et al. [11], a calibration specimen, having diameter and material properties identical to those of the incident and transmitter bars, is used instead of a real specimen. With the calibration specimen, the effect of the specimen size and the mechanical properties on the stress transmitting characteristics can be excluded, and the effect on the wave propagation of only the thread can be investigated. The strain at the transmitter bar is compared with that at the incident bar for various thread conditions. For the accurate measurement of the stress and strain of the threaded specimen, the stress wave, when a calibration specimen is used, should not be distorted in the thread region and the strains at the incident and transmitter bars should be the same [11]. The effect of the thread shape and the yield stress of the calibration specimen on the stress transmit characteristics is investigated. Finally, a design guide for thread and striker velocity is proposed to reduce the wave distortion in the thread region.

## 2. Principle of tensile split Hopkinson bar system

### 2.1. Tensile split Hopkinson bar system and accuracy issues

Fig. 1 provides a schematic illustration of the SHTB system. A striker tube is fired to impact an anvil. From the impact, a tensile pulse is generated in the incident bar and propagated to the specimen. Part of the incident pulse is transmitted to the specimen and propagates through a transmitter bar as a tensile pulse. The rest of the pulse reflects to the incident bar as the compressive pulse. The transmitted and reflected pulses are measured at the points to which strain gages have been attached on the two bars at equal distances from each end of the bars. The transmitted and reflected pulses are used to calculate the stress and strain in the specimen according to

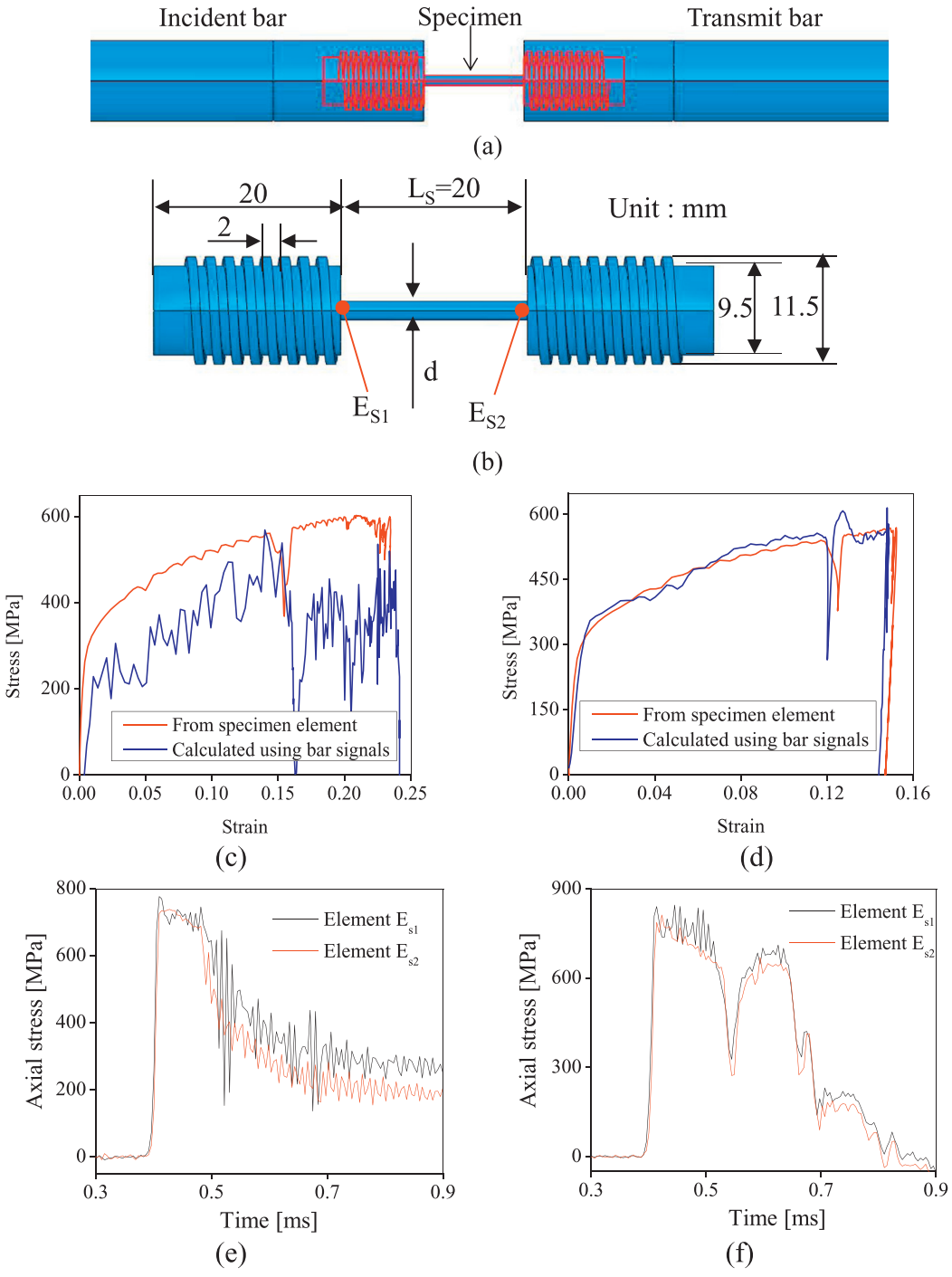


**Fig. 2.** Examples of measurement error: (a) schematic illustration of screw fixing, (b) dimensions of specimen, (c), (d) comparison of the calculated (using the incident and transmitter bar strain) stress-strain relation with that monitored form the specimen for specimen diameters of 2.0 and 8.0 mm, respectively, and (e), (f) axial stress at elements $E_{S1}$ and $E_{S2}$ for specimen diameters of 2.0 and 8.0 mm, respectively.

the following equation:

$$\sigma(t) = \frac{A_o}{A} E_o \varepsilon_T(t) \quad (1)$$

$$\varepsilon(t) = -2\frac{C}{L_s}\int_0^t \varepsilon_R(\tau)d\tau. \quad (2)$$

In Eqs. (1) and (2), $E_O$ is the elastic modulus of the bars. $A_O$ and A are the areas of the bar and the specimen, respectively. $\varepsilon_T$ and $\varepsilon_R$ are the transmitted and reflected strains measured at the transmitter and incident bars, respectively. C is the wave speed and $L_s$ is the specimen length. Eqs. (1) and (2) were derived with assumptions of one-dimensional wave propagation and contact condition of specimen with bars. As mentioned in chapter 1, the equilibrium of SHTB system was checked by measuring the stress signal at specimen ends ($E_{S1}$ and $E_{S2}$ in Fig. 2(b)) and the results are shown in Fig. 2(e) and (f). As can be seen in Figs. 2(e) and (f), the strain signals at $E_{S1}$ and $E_{S2}$ are almost same, so the Eqs. (1) and (2) are sufficient for one-dimensional wave propagation condition of SHTB system. In

addition, the contact condition means the velocity and displacement of the specimen end should be the same as that of the bar end. In the compressive SHPB test, the contact condition is usually satisfied during compressive deformation of the specimen. In the SHTB test, however, due to wave propagation through the thread, the displacement of the specimen ends ($E_{S1}$ and $E_{S2}$ in Fig. 1) is not the same as the displacement of the bar ends ($E_{B1}$ and $E_{B2}$ in Fig. 1). For example, if severe plastic deformation takes place on the thread or specimen outside measured specimen $L_s$, the displacement of the specimen end will be different from that of the bar end and error will be included in the measured results. The aim of this study is to investigate the effect of the thread of the specimen and of the bars on the stress wave propagation characteristics. As a result, a thread shape is proposed to minimize the wave propagation error.

### 2.2. Bars and calibration specimen description

To investigate the effect of threads of the specimen and bars on wave propagation error, a calibration specimen is used instead of a real specimen. Fig. 3 provides a schematic illustration of the SHTB calibration apparatus and a detailed view of the threaded calibration specimen. The lengths of the incident and transmitter bars are 2000 mm and the diameter is 16 mm. The diameter of the calibration specimen is identical to the diameter of the incident and transmitter bars. In the calibration SHTB apparatus, the bars and threaded cylindrical calibration specimen are joined together directly. When the bars and the identical sized calibration specimen are assembled, the two bars, along with the calibration specimen, have to behave as a single continuous bar. This means that the strains at the incident and transmitter bars should be the same and no stress can be reflected at the thread boundaries. Two types of thread shape, i.e., rectangular and triangular threads, are subjected to analysis. Fig. 4 shows the meshes of the two types of specimen shape. First, the thread shape and pitch were determined to obtain a minimum value of strain error. Then, to investigate the wave transmitting characteristics of the thread region, various tests were performed numerically for different thread inner diameters, yield stresses of the calibration specimen, and striker velocities.

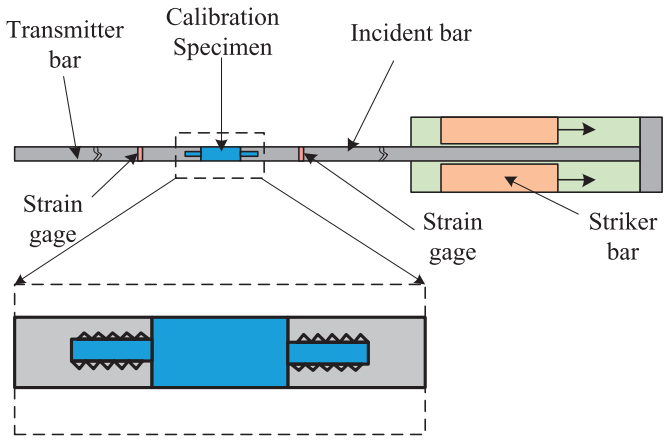


**Fig. 3.** Schematic illustration of SHTB calibration apparatus and detailed view of threaded calibration specimen area.

When the stress wave was transmitted perfectly without loss, the strains at the incident and transmitter bars should be the same. Therefore, the average strain error ratio is used to compare the difference between the incident and transmitted strain signals. The average strain error ratio is calculated using the

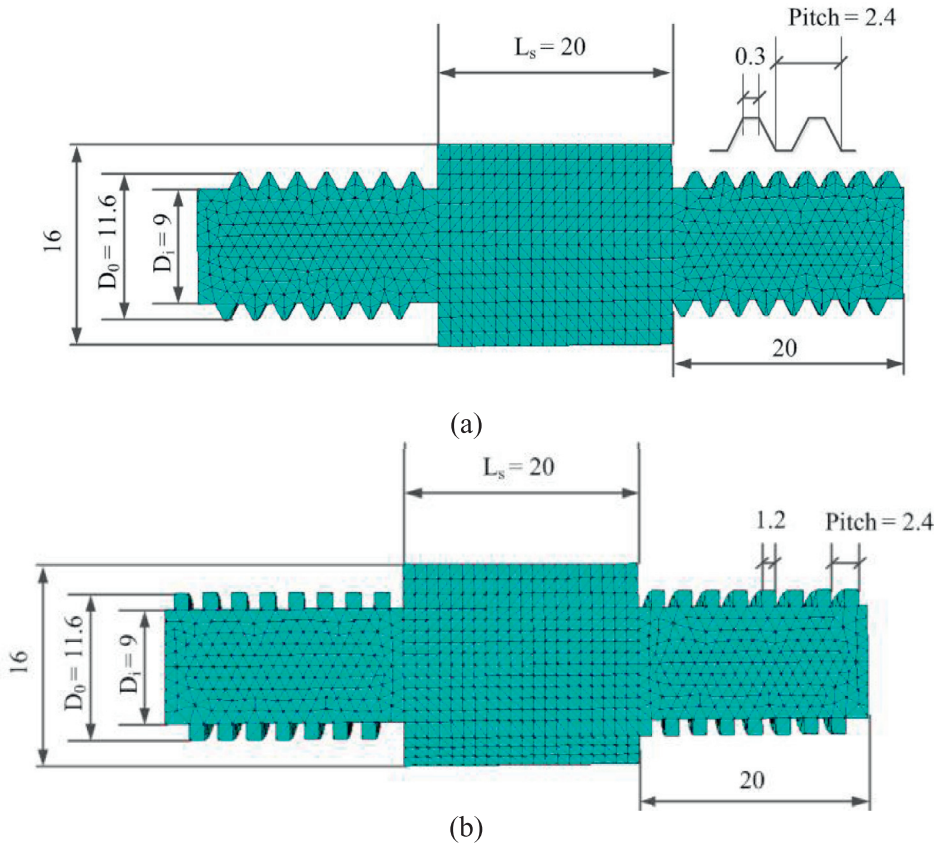


**Fig. 4.** Element discretization and dimensions for (a) triangular and (b) rectangular thread specimen.

following equation:

$$\lambda_{\varepsilon} = \frac{\sum_{k=0}^{n} \left| \varepsilon_{Ik} - \varepsilon_{Tk} \right|}{\sum_{k=0}^{n} \varepsilon_{Tk}} \tag{3}$$

where $\varepsilon_{Ik} - \varepsilon_{Tk}$ is the difference between the incident strain $\varepsilon_I$ and the transmitted strain $\varepsilon_T$ at the sampling point k, and n is the total number of sampling points within the strain pulse.

In this paper, the Johnson-Cook constitutive relation of AISI 4340 steel is applied to the calibration specimen and bars material. The John-cook constitutive model describes the plastic flow stress by the relation,

$$\overline{\sigma} = (A + B\bar{\varepsilon}^{n})(1 + C\ln(\dot{\bar{\varepsilon}}/\dot{\bar{\varepsilon}}_0)(1 - T^{*m}) \tag{4}$$

where A, B, n, C, and m are material constants, $\bar{\varepsilon}$ is the equivalent plastic strain, $\dot{\bar{\varepsilon}}$ is the equivalent plastic strain rate, $\dot{\bar{\varepsilon}}_0$ is the reference strain rate, and $T^*$ is the homologous temperature given by Eq. (5).

$$T^{*} = \frac{T - T_{room}}{T_{melt} - T_{room}} \tag{5}$$

where T is the temperature of the specimen, and $T_{melt}$ is the melting temperature of the specimen. The Johnson-Cook equation contains five material constants, A, B, n, C, and m. The first bracket in Eq. (4) indicates a strain hardening term. The second bracket indicates a strain rate hardening term, and the third bracket is a thermal softening term. The five constants in the Johnson-Cook constitutive relation for AISI 4340 steel are shown in Table 1 [19].

## 3. Results and discussion

### 3.1. Effect of specimen thread type on calibration results

In the SHTB system, the thread shape and pitch of the specimen and bars affect the stress wave propagation from the incident to the transmitter bars through the specimen; therefore, the simulation of thread is necessary and very important. To investigate the effects of the thread on the wave propagation, calibrations were performed and analyzed numerically using calibration specimens having two thread types, i.e., rectangular and triangular threads, as shown in Fig. 4. Fig. 5 shows the deformed shape and von-Mises stress of the rectangular and the triangular thread specimens when a stress wave passed through the thread region. The inner diameter is 9.0 mm and the striker velocity is 20 m/s. Very high stress is shown in the thread region. Analyses were carried out for various pitches and the average strain error ratio was calculated using Eq. (3). The thread length was fixed at 20 mm. Therefore, the number of threads varies as the pitch changes. Fig. 6 shows the incident and transmitted strains for the triangular and rectangular thread specimens, and the average strain error ratio for various values of thread pitch. In Fig. 6(a) and (b), it can be seen that the transmitted strains are very different from the incident strain. Fig. 6(c) shows the calculated average strain error ratios for two thread types. It can be clearly seen that the average strain error ratio when using rectangular thread is much lower than that when using triangular thread. Also, it is shown that the thread shape and pitch have an effect on the wave transmit capability through the thread. Based on these results, the rectangular thread with 2.4 mm pitch was chosen for the next analysis.

**Table 1**
Material properties of AISI 4340 steel.

| Property | | Value |
|---|---|---|
| Density | | 7865 kg/m$^3$ |
| Young's modulus | | 200 GPa |
| Poisson's ratio | | 0.285 |
| Johnson–Cook [20] model coefficients | A | 792 MPa |
| | B | 510 MPa |
| | C | 0.014 |
| | n | 0.26 |
| | m | 1.03 |
| | $T_m$ | 1700 K |

### 3.2. Effects of thread inner diameter on calibration results

To investigate the effect of the inner diameter of the thread, calibration tests were performed for various inner thread diameters. Fig. 7 shows the deformed shape and von-Mises stress distribution of rectangular threads with inner diameters of 5, 7, 9, and 11 mm. In the analysis, the thread height and pitch were fixed at 2.0 and 2.4 mm, respectively. The striker velocity was 20 m/s. The maximum stress decreases as the inner diameter increases. When the inner diameters were 5 and 7 mm, local necking and severe plastic deformation took place. Fig. 8 shows the strain signals monitored at the incident and transmitter bars for different inner diameters of the thread. The strain-time curves at the incident bar are same for all of analysis cases. The strain-time curves at the transmitter bar, however, are very different. For perfect transmission of the stress wave through the thread, the strain-time curves at the incident and transmitter bars should be the same. In Fig. 8, it can be clearly seen that the inner diameter of the thread affects the stress wave propagation; there is a great discrepancy between the strains at the transmitter and incident bars and between the strains at the transmitter bars with different inner diameters of specimen thread. Fig. 9 shows the average strain error ratio calculated according to Eq. (3). When the inner diameter was 9 mm, the average strain error ratio was at a minimum. When the thread inner diameter was smaller than 9 mm, the average strain error ratio became very high. The severe plastic deformation in the thread region is considered to be the main cause of the error. To investigate the reason for the error increase when the inner diameter is 11.0 mm, the deformed shape and the von-Mises stress of the incident bar end are shown in Fig. 7(e) and (f). When the inner diameter of the thread is 11.0 mm, the outside thickness of the bar end becomes very small and severe plastic deformation takes place. This means that sufficient tensile force cannot be transferred to the calibration specimen, which causes error. In this

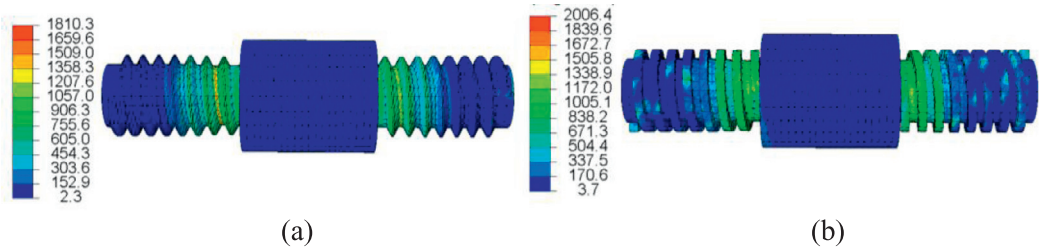


**Fig. 5.** Deformed shape and von-Mises stress distribution for (a) triangular and (b) rectangular thread specimen.

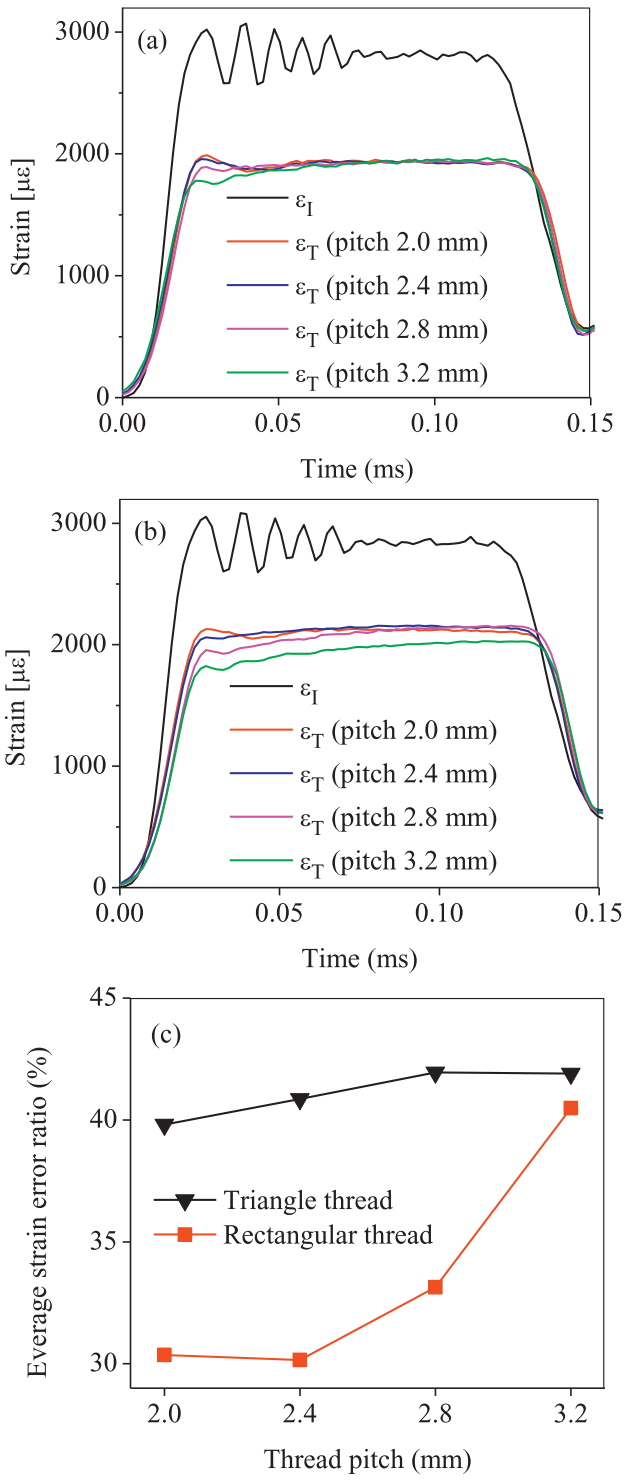


**Fig. 6.** Incident strains ($\varepsilon_I$) and transmitted strains ($\varepsilon_T$) for (a) triangular and (b) rectangular thread, and (c) averaged strain error ratio for various pitches.

calibration test, therefore, it is shown that the inner diameter of the thread has a great effect on the stress wave transmission. Under these test conditions, the calibration specimen of 9.0 mm inner diameter yields the best results.

Until now, the effects of the thread shape, pitch, and inner diameter on the wave transmit characteristics have been investigated. Optimum thread shapes may be different for different specimen materials and different specimen diameters and lengths. So, the optimization of the thread shape is not carried out and just the effects of the thread shapes on the wave transmit characteristics are investigated. A detailed study of error causes is carried out in the next section.

### 3.3. Effect of static yield stress on calibration results

Even when the thread shape and inner diameter are determined properly for the calibration specimen, there is still some discrepancy between the strain signals at the incident and transmitter bars. To investigate in detail the stress wave transmitting characteristics through the thread, analysis is carried out for various yield strengths, i.e., values of coefficient A of the Johnson-Cook model. Fig. 10 shows the deformed shape and effective plastic strain of the threaded calibration specimen for various values of coefficient A of the Johnson-Cook constitutive model [20]. The striker velocity is 20 m/s, the thread pitch is 2.4 mm, and the inner diameter of thread is 9.0 mm. The maximum effective plastic strain in the thread region decreases as the yield strength increases. Fig. 11 shows the strain-time curve at the incident and transmitter bars for various values of yield strength. As the yield strength increases the discrepancy between the strains at the incident and transmitter bars and finally, the strain-time curves at the incident and transmitter bars become almost identical when the material is assumed to be elastic. Fig. 12 shows the correlation between the yield strength, average strain error ratio, and maximum equivalent plastic strain. It can be seen that the average strain error ratio is highly dependent on the yield strength of the bars and that the strain error decreases with the yield strength. The strain error is also highly dependent on the plastic deformation of the thread region. As the maximum equivalent plastic strain decreases, a more perfect stress wave can be transmitted from the incident bar to the transmitter bar without wave distortion. In test conditions of 20 m/s striker velocity and calibration specimen of diameter and material identical to those of the incident bar, the incident stress wave can be considered to pass without severe loss to the transmitter bar when the yield stress of the bar and specimen are greater than or equal to 1500 MPa (Fig. 11). The yield strength of the bar materials such as maraging steel is greater than 1500 MPa. However, the yield strength of the general specimen materials such as copper is far lower than 1000 MPa. Therefore, the SHTB test should be carried out considering the stress wave transmitting capability of the thread, depending on the shape, inner diameter, pitch, and yield strength of the thread.

### 3.4. Effect of striker velocity on calibration results

To determine the striker velocity that guarantees accurate wave transmission from the incident bar to the transmitter bar, analyses were carried out for various striker velocities. Fig. 13 shows the deformed shape and von-Mises stress distribution of the calibration specimen for various striker velocities. The pitch, inner diameter, and thread height of the thread are 2.4 mm, 9.0 mm, and 2.0 mm respectively. The material properties of the bar and the calibration specimen are listed in Table 1. When the striker velocity is lower than or equal to 7.0 m/s, the maximum von-Mises stresses are almost the same. When the striker velocity is greater than 7.0 m/s, the maximum von-Mises stress increases as the striker velocity increases. Local necking is shown when the striker velocities are 30.0 and 40.0 m/s. Fig. 14 shows the strain-time curves at the incident and transmitter bars for the various striker velocities. When the striker velocity is lower than or equal to 10.0 m/s, the strains at the incident and transmitter bars are almost the same. However, the strain difference

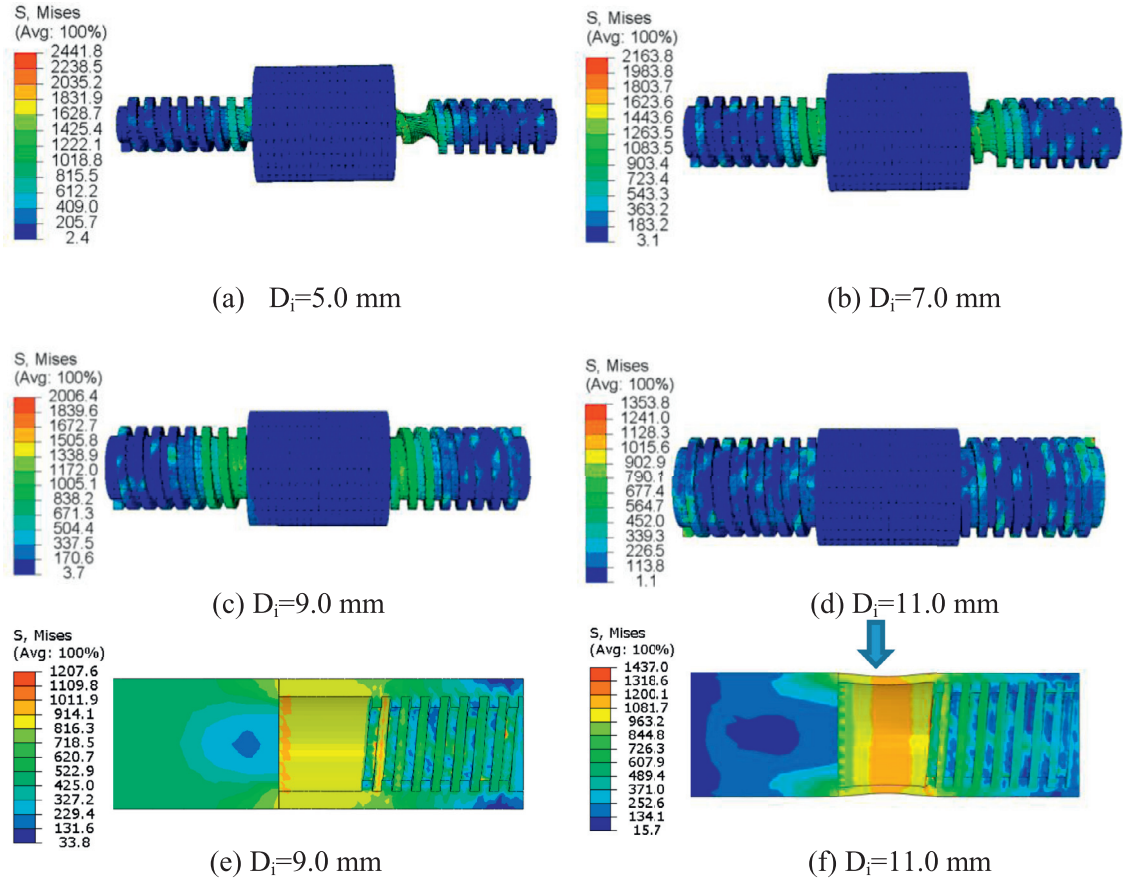


**Fig. 7.** Deformed shape and von-Mises stress distribution on the calibration specimen ((a)–(d)) and incident bar end ((e) and (f)).

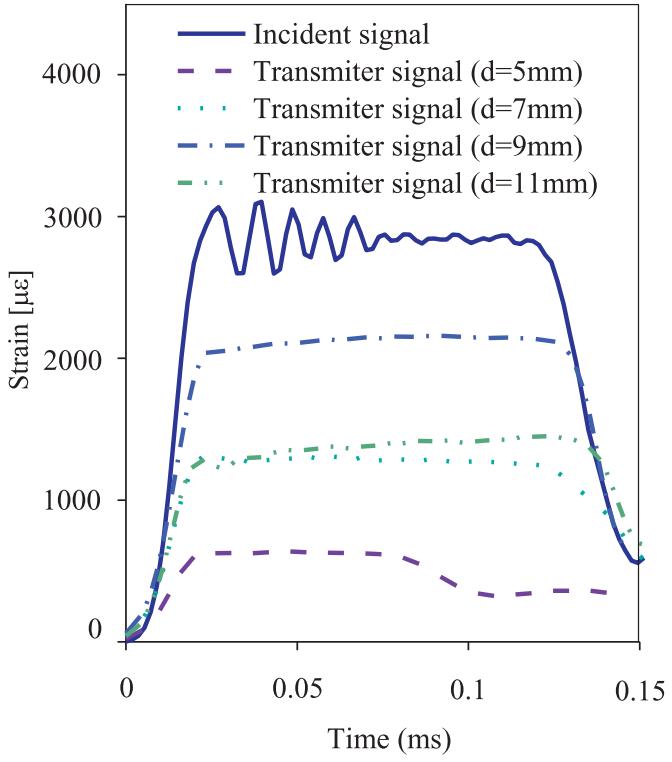


**Fig. 8.** Incident and transmit strains for various inner diameters.

between the incident and the transmitter bars becomes severe when the striker velocity is greater than 10.0 m/s; this difference increases as the striker velocity increases.

The strain difference values between the incident and transmitter bars are summarized in Fig. 15. Fig. 15 shows the correlation between the average strain error ratio, the ratio of the maximum von-Mises stress to yield strength, and the striker

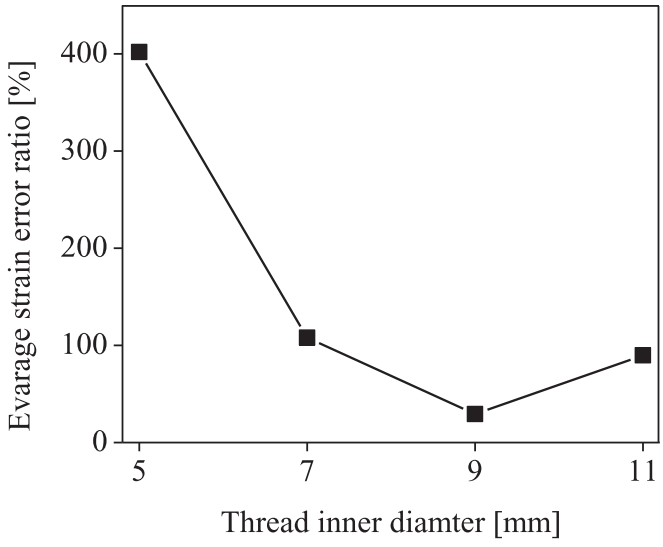


**Fig. 9.** Average strain error ratio for various inner diamters.

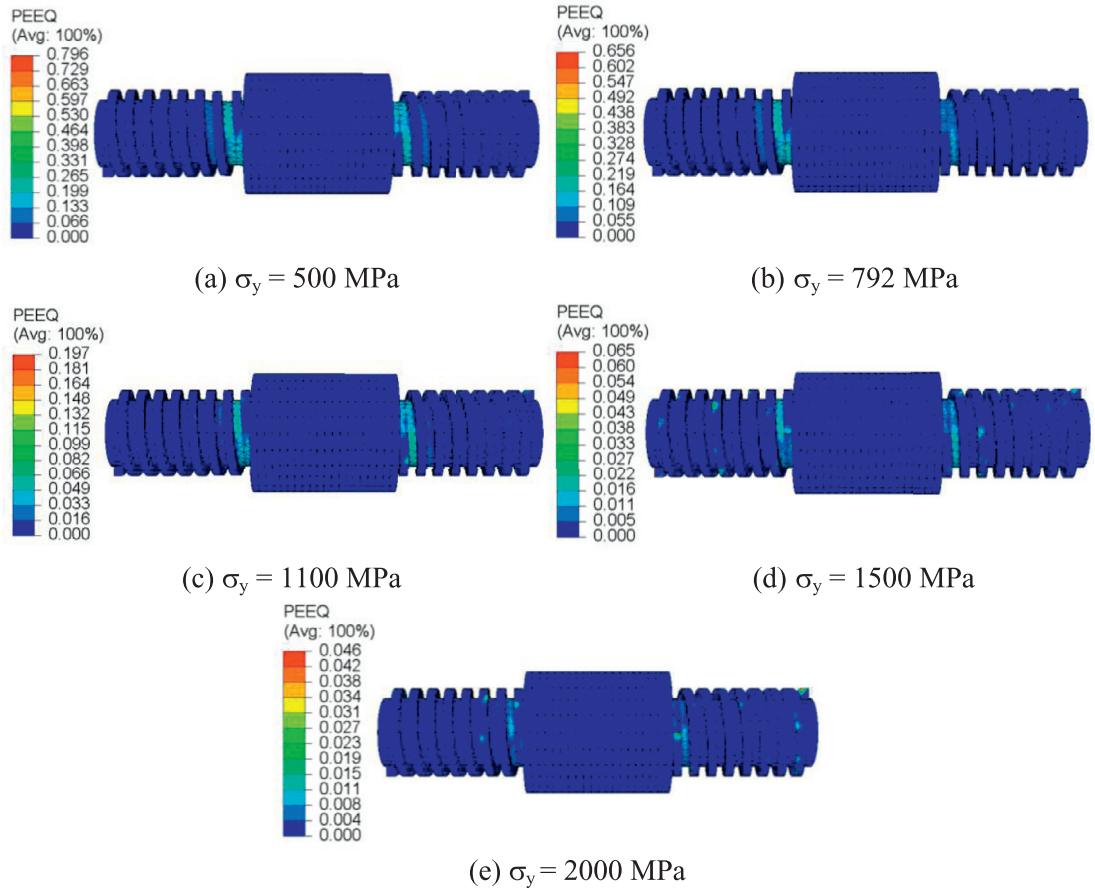


**Fig. 10.** Deformed shape and equivalent plastic strain of specimen for various yield strengths.

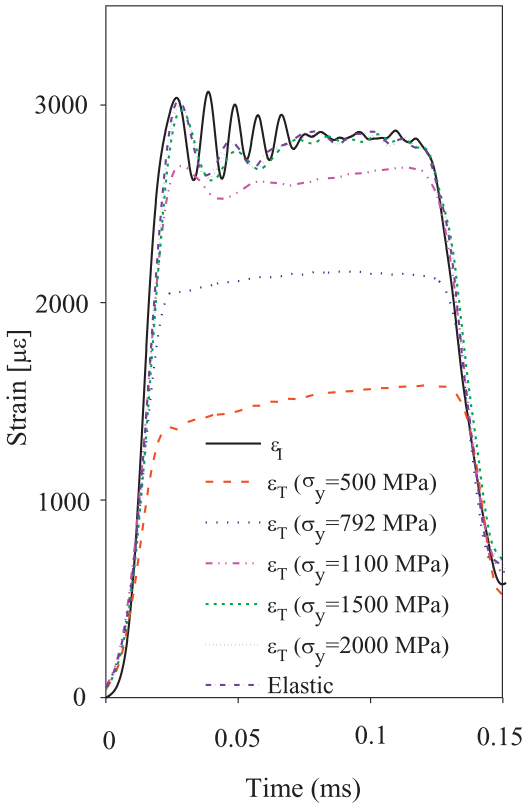


**Fig. 11.** Comparison of the strain-time curves at incident and transmitter bars for various yield strength.

velocity. The ratio of the maximum von-Mises stress to yield strength is defined as:

$$\eta = \frac{\sigma_{max}}{\sigma_y} \tag{6}$$

where $\sigma_{max}$ is the maximum von-Mises stress measured at the specimen and $\sigma_y$ is the static yield stress (coefficient A of Johnson-Cook model) of the specimen.

It is clearly shown that the average strain error ratio drops when the striker velocity is low and the stress ratio, $\eta$, is small. In these

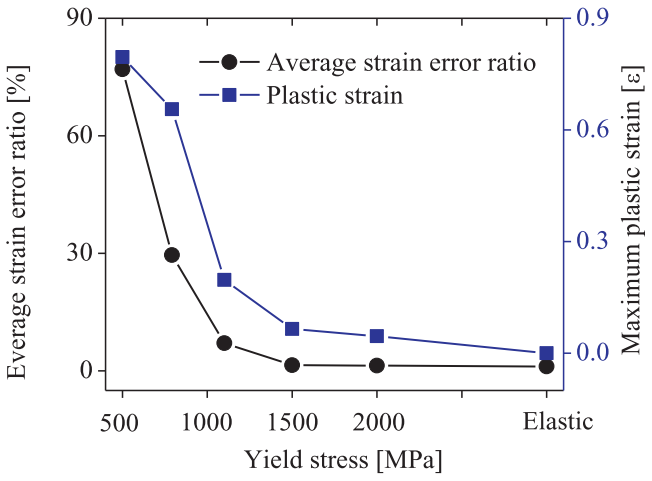


**Fig. 12.** Effect of material yield stress on average strain error ratio and the maximum plastic strain in the specimen.

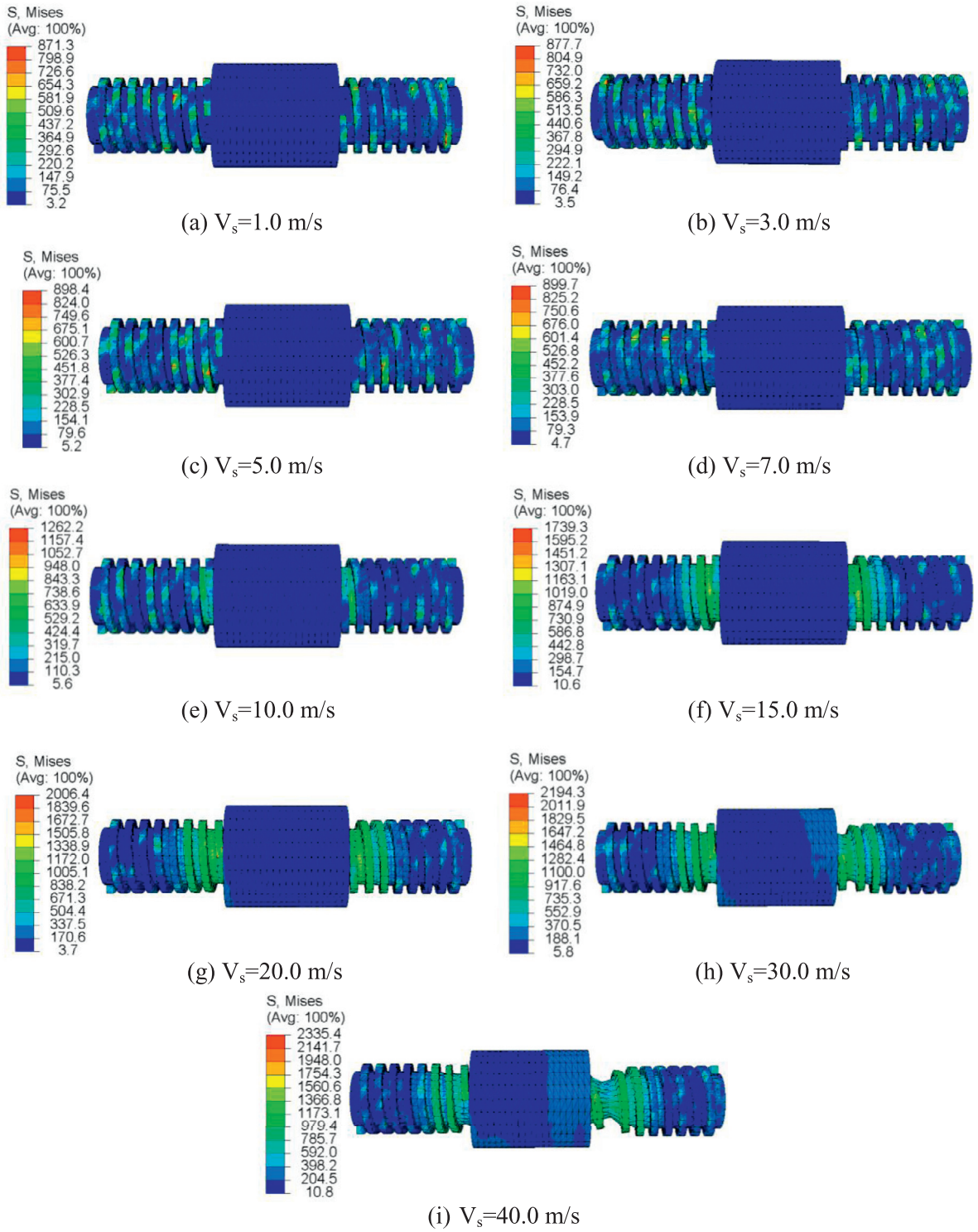


**Fig. 13.** Deformed shape and von-Mises stress distributions for various striker velocities.

test conditions, with the calibration specimen, the incident stress wave can be accurately transmitted to the transmitter bar through the threaded specimen when the striker velocity is lower than or equal to 10 m/s. Also, the wave transmission capability is strongly dependent on the plastic deformation of the thread. It is certain that the specimen has different dimensions and mechanical properties from those of the calibration specimen. To understand the wave propagation capability of the thread shape by excluding other factor affecting the wave propagation, a calibration specimen with outer diameter and mechanical properties identical to those of the bars is used. The plastic deformation in the thread region is highly dependent on the force needed for plastic deformation in the specimen region. Therefore, the specimen for the SHTB test should be designed to satisfy the condition of no plastic deformation of the thread region when the specimen region deforms plastically.

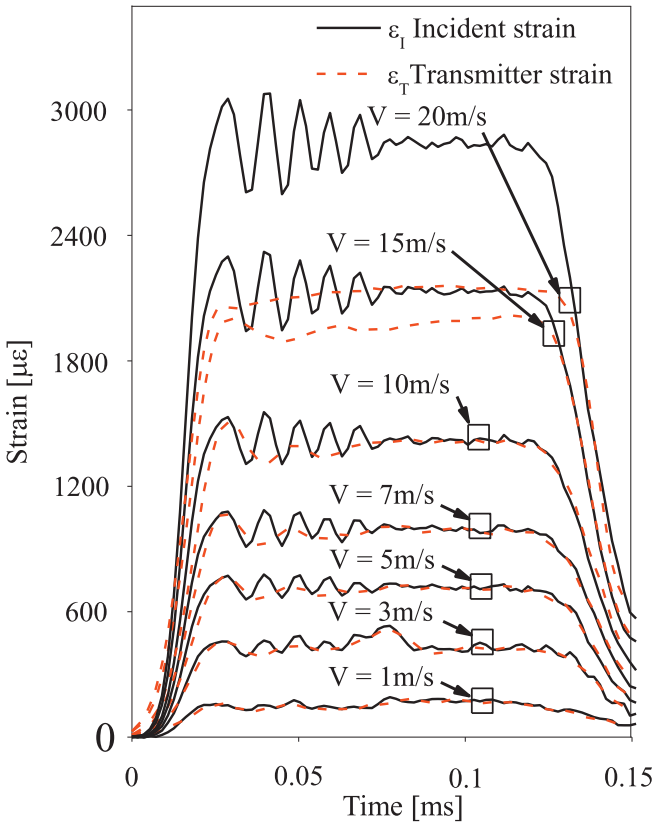


**Fig. 14.** Incident and transmitted strains at different level of striker velocity from 1 m/s to 20 m/s.

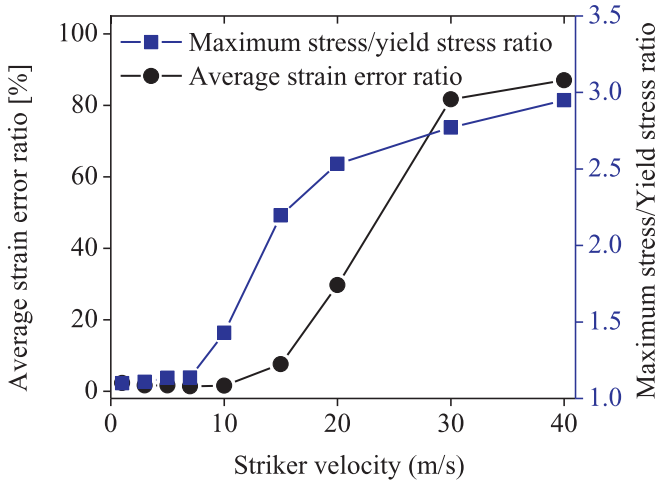


**Fig. 15.** Effect of striker velocity and maximum stress/yield stress ratio on the average strain error ratio.

## 4. Conclusion

The stress wave transmission characteristics through threading in the SHTB test are investigated using a calibration specimen. Through finite element analysis for various thread shapes and striker velocities, the following conclusions were obtained.

1. The thread shapes, such as triangular and rectangular shape, have great effects on the wave transmitting capability of the thread.
2. Strain error between the incident and transmitter bars is defined; we investigated the relation between the strain error and the maximum plastic strain in the thread region, and also the ratio of the maximum von-Mises stress to the yield stress. It has been clearly shown that the strain error is highly dependent on the maximum plastic strain in the thread region and on the ratio of the maximum von-Mises stress to the yield stress. As the maximum plastic strain in the thread region increases, the strain discrepancy at the incident and transmit bars increases.
3. As a result, the plastic deformation in the thread region depends on the striker velocity and strain rate. It is shown that the specimen for the SHTB test should be designed to satisfy the condition of no plastic deformation in the thread region while the specimen region (inside gage point, $L_s$ in Fig. 1) deforms plastically. If it is impossible to design the thread to deform in the pure elastic region, the thread should be designed to at least minimize the plastic deformation. A good specimen design depends not only on the material, geometry but also boundary conditions, such as striker velocity and target nominal strain rate.

## Acknowledgments

This work was supported by the National Research Foundation of Korea (NRF) grant funded by the Korean Government (Ministry of Education) (No. NRF-2016R1D1A1B01014711) and by the research fund of the Survivability Technology Defense Research Center of the Agency for Defense Development of Korea (No. UD090090GD).

## References

[1] Kolsky H. An investigation of the mechanical properties of materials at very high rates of loading. Proc Physical Soc B 1949;62(11):676–700.
[2] Duffy J, Campbell JD, Hawley RH. On the use of a torsional split Hopkinson bar to study rate effects in 1100-0 Aluminum. J Appl Mech 1971;38(1):83–91.
[3] Harding J, Wood EO, Campbell JD. Tensile testing of materials at impact rates of strain. J Mech Eng 1960;2:88–96.
[4] Hauser F. Techniques for measuring stress-strain relations at high strain rates. Exp Mech 1966;6(8):395–402.
[5] Ogawa K. Impact-tension compression test by using a split-Hopkinson bar. Exp Mech 1984;24(2):81–6.
[6] Lindholm US, Yeakley LM. High strain-rate testing: Tension and compression. Exp Mech 1968;8(1):1–9.
[7] Huh H, Kang WJ, Han SS. A tension split Hopkinson bar for investigating the dynamic behavior of sheet metals. Exp Mech 2002;42(1):8–17.
[8] Pham TN, Choi HS, Kim JB. A numerical investigation into the tensile split Hopkinson pressure bars test for sheet metals. Appl Mech Mater 2013;421:464–7.
[9] Nicholas T. Tensile testing of materials at high rates of strain. Exp Mech 1981;21(5):177–85.
[10] Naik N K, Perla Y. Mechanical behaviour of acrylic under high strain rate tensile loading. Polymer Testing 2008;27(4):504–12.
[11] Pothnis JR, Perla Y, Arya H, Naik NK. High strain rate tensile behavior of aluminum alloy 7075 T651 and IS 2062 mild steel. J Eng Mater Technol 2011;133(2):021026.
[12] Vilamosa V, Clausen AH, Borvik T, Skjervold SR, Hopperstad OS. Behaviour of Al-Mg-Si alloys at a wide range of temperatures and strain rates. Int J Impact Eng 2015;86:223–39.
[13] Haugou G, Markiewicz E, Fabis J. On the use of the non direct tensile loading on a classical split Hopkinson bar apparatus dedicated to sheet metal specimen characterization. Int J Impact Eng 2006;32:778–98.
[14] Fransplass H, Langseth M, Hopperstad OS. Tensile behavior of threaded steel fasteners at elevated rates of strain. Int J Mech Sci 2011;53:946–57.
[15] Fransplass H, Langseth M, Hopperstad OS. Experimental and numerical study of threaded steel fasteners under combined tension and shear at elevated loading rates. Int J Impact Eng 2015;76:118–25.
[16] Chen Y, Clausen AH, Hopperstad OS, Langseth M. Stress–strain behaviour of aluminium alloys at a wide range of strain rates. Int J Solids Struct 2009;46:3825–35.

[17] Chen Y, Clausen AH, Hopperstad OS, Langseth M. Application of a split-Hopkinson tension bar in a mutual assessment of experimental tests and numerical predictions. Int J Impact Eng 2011;38:824–36.
[18] Chen W, Song B. Split Hopkinson (Kolsky) bar: design. Testing and applications. New York, USA: Springer; 2011.
[19] Owolabi G, Odoh D, Odeshi A, Whitworth H. Occurrence of dynamic shear bands in AISI 4340 steel under impact loads. World J Mech 2013;3:139–45.
[20] Johnson GR, Cook WH. A constitutive model and data for metals subjected to large strains, high strain rates and high temperatures. In: Proceedings: 7th international symposium on ballistics, The Hague; 1983. p. 541–7.